

Challenges and Opportunities in Improving Worst-Group Generalization in Presence of Spurious Features

Siddharth Joshi¹Yihao Xue^{*1}Yu Yang^{*1}Wenhan Yang^{*1}Baharan Mirzasoleiman¹¹Department of Computer Science, UCLA, Los Angeles, CA, 90024

Abstract

Deep neural networks often exploit (*spurious*) features that are present in the majority of examples within a class during training. This leads to *poor worst-group test accuracy* i.e. poor accuracy for minority groups that lack these spurious features. Despite the growing body of recent efforts to address spurious correlations (SC), several challenging settings remain unexplored. In this work, we propose studying methods to mitigate SC in settings with 1) spurious features that are learned more slowly, 2) a larger number of classes and 3) a larger number of groups. We introduce two new datasets, SPUCOANIMALS and SPUCOSUN, to facilitate this study and conduct a systematic benchmarking of **8** state-of-the-art (SOTA) methods across a total of **5** vision datasets, training over **5K** models. Through this, we highlight how existing group inference methods struggle in the presence of spurious features that are learned later in training. Additionally, we demonstrate how all existing methods struggle in settings with more groups and/or classes. Finally, we show the importance of careful model selection (hyperparameter tuning) in extracting optimal performance, especially in the more challenging settings we introduced, and propose more cost-efficient strategies for model selection. Overall, through extensive and systematic experiments, this work uncovers a suite of new challenges and opportunities for improving worst-group generalization in the presence of spurious features.

1 INTRODUCTION

Overparameterized machine learning models can be highly accurate on average, yet consistently fail on atypical or minority groups of the data. These performance disparities across groups can be especially pronounced in the presence of spurious correlations, i.e. features that exist in majority of examples of a class in training data but not in test data.

There has been a lot of recent efforts to address this problem. If groups of examples with the spurious features are known, robust training methods such as group balancing Idrissi et al. [2022a] or group distributionally robust optimization (GDRO) Sagawa* et al. [2020], upsample or upweight the minority groups to mitigate the spurious correlations. If group labels are not available, existing methods first infer majority and minority groups and then apply robust training to mitigate the spurious correlations Yang et al. [2024], Liu et al. [2021], Creager et al. [2021].

Nevertheless, existing evaluations are limited to very simplistic scenario of binary classification with spurious features that are learned very early during training. In particular, standard benchmark datasets for this problem are Waterbirds Sagawa* et al. [2020] and CelebA Liu et al. [2015], both with two classes and two groups in each class, where the majority group contains a simple spurious feature that is learned very early during the training.

In this work, we study the effectiveness of existing methods in previously unexplored settings, i.e., spurious features that are not learned very early during the training and multi-class classification with multiple groups per class. To do so, we introduce two new datasets, namely SPUCOSUN and SPUCOANIMALS, each with four classes and one spurious feature per class, with 16 and 8 groups, respectively. For SPUCOSUN, we present two versions, SPUCOSUN (Fast) and SPUCOSUN, to contrast datasets where the spurious feature is learned early versus later during training. Then, we benchmark 8 state-of-the-art methods on our datasets, in addition to Waterbirds, CelebA, and the more recently

^{0*} = Equal contribution.

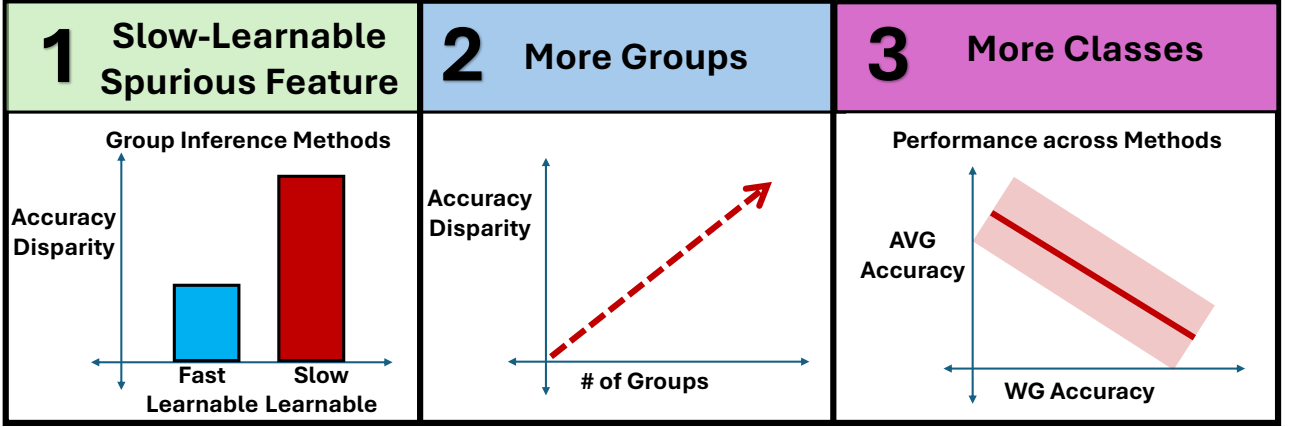


Figure 1: Larger accuracy disparity is worse. 1) Slow-learnable spurious features are more challenging for group inference methods. 2) More groups are more challenging for all methods 3) More classes make it challenging to maintain high AVG while improving WG accuracy (seen as a strong negative correlation between AVG and WG and a large spread across methods)

introduced UrbanCars Li et al. [2023] (all with 2 classes).

By training over 5K models, we reveal challenges and opportunities for future research in this direction (summarized in Fig. 1:

- When the spurious feature is learned later, group inference methods struggle to infer groups accurately
- Existing methods struggle to bridge the gap between worst-group and average accuracy (accuracy disparity) in presence of more groups in the data.
- With the same number of groups, when data has more classes, maintaining high average accuracy while improving worst-group accuracy is more challenging
- Model selection is crucial for methods to mitigate SC, especially in the presence of more groups & classes
- Model selection for group inference methods is extremely expensive and can be made $\approx 100\times$ cheaper by directly evaluating the quality of inferred groups

The insights from our study can inspire future research to develop more robust solutions to the critical challenge of improving worst-group accuracy due to spurious features.

2 RELATED WORK

Spurious correlation. Spurious correlations occur when a feature is spuriously linked to a class (e.g., dogs often wearing collars, cats typically not), leading to low test accuracy on minority groups (e.g., cats with collars or dogs without). Mitigating models’ reliance on spurious correlations can also improve out-of-distribution generalization by encouraging the model to focus on generalizable features (e.g., the

true characteristics of a dog) rather than spurious features (e.g., the collar). However, our paper specifically focuses on mitigating spurious correlations in the context of improving worst-group (WG) accuracy, rather than addressing spurious correlations in general or other scenarios like domain generalization Gulrajani and Lopez-Paz [2020a], Zhang et al. [2023] (see Fig. 2 for an illustration of the difference between the spurious correlation and domain generalization settings) or other natural distribution shifts Hendrycks et al. [2021a,b], Taori et al. [2020]. Improving WG accuracy has been a central objective in a rich body of research on spurious correlations Liu et al. [2021], Yang et al. [2024], Nam et al. [2022], Kirichenko et al. [2023], Idrissi et al. [2022a], Sagawa* et al. [2020], Deng* et al. [2023].

Existing Datasets. There are many existing datasets that focus on domain generalization. For example, DomainBed Gulrajani and Lopez-Paz [2020a] focuses exclusively on studying domain generalization, and the majority of datasets in WILDS Koh et al. [2021] are also designed for this purpose. Other datasets, including NooCh Madras and Zemel [2021], NICO He et al. [2021], and ImageNet-X Idrissi et al. [2022b], are primarily designed as test sets for evaluating domain generalization, focusing on model performance on unseen domains rather than addressing the spurious correlations setting. Even when spurious correlations are considered, existing datasets often fail to capture challenging settings, such as a large number of groups, multiple classes, or spurious features learned later in training, which we show are indeed difficult even for current SOTA methods. For example, the datasets in WILDS addressing spurious correlations, such as Waterbirds and CelebA, are limited to only 2 classes and 4 groups, which restricts their effectiveness in evaluating models on more complex spurious correlation

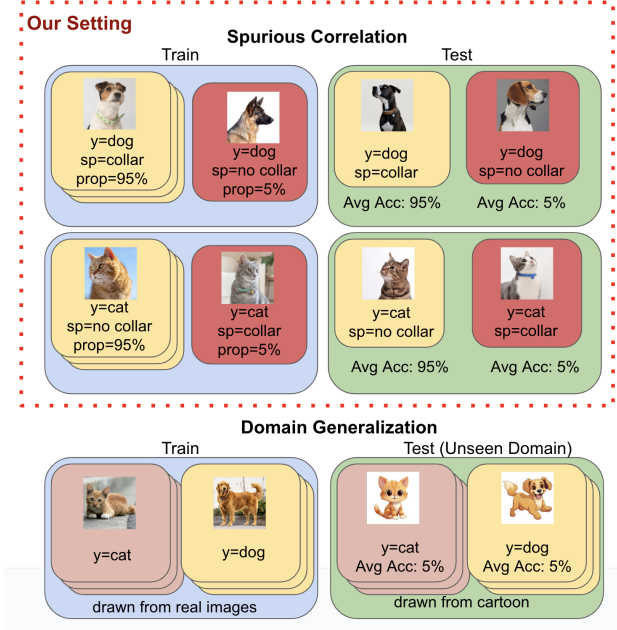


Figure 2: Our Setting (Top): In spurious correlations, certain features (e.g. collar) are spuriously correlated with specific classes (dogs) e.g. Majority of dogs appear with collars and cats without collars, hence collars are spuriously correlated with dogs. Bottom: In domain generalization, we train on one domain (e.g., real images) and test on unseen domains (e.g., cartoon images).

challenges. Datasets like bFFHQ Kim et al. [2021] and BAR Nam et al. [2020] have the same limitations and also exclude certain groups from validation, further reducing their utility for assessing SOTA methods (these rely heavily on model selection using the validation set). Recently, Li et al. [2023] proposed UrbanCars to study spurious correlations, a dataset with 8 groups, addressing the small # of groups in previous datasets. In contrast to prior work, this paper centers on spurious correlations and introduces datasets with greater complexity: 8-16 groups, 4 classes. Additionally, we also consider settings with fast and slow-learnable spurious features. Our findings reveal significant limitations in current SOTA methods when addressing these complex scenarios.

Existing Benchmarks The recent work by Yang et al. Yang et al. [2024] proposes a general framework for subpopulation shifts, including spurious correlations. However, their evaluation is limited, considering only three methods in spurious correlation settings, and their datasets (i.e., WILDS and CelebA) are less challenging. In comparison, our benchmark provides a comprehensive analysis of **8 SOTA methods** across **5 vision datasets**, specifically designed to include more groups, more classes, and more challenging spurious features. This extensive evaluation highlights the challenges that remain in mitigating spurious correlations.

3 BACKGROUND

Let $\mathcal{D} = \{(\mathbf{x}_i, y_i)\}_{i=1}^n$ be the training data with input features $\mathbf{x}_i \in \mathbb{R}^d$ and labels $y_i \in [\mathcal{C}]$.

Machine learning models are trained by minimizing an empirical risk function (ERM) using (stochastic) gradient descent. The goal of ERM is to minimize the average error on the entire training data \mathcal{D} :

$$\mathbf{w}^* \in \arg \min_{\mathbf{w}} \mathbb{E}_{(\mathbf{x}_i, y_i) \in \mathcal{D}} [l(f(\mathbf{w}, \mathbf{x}_i), y_i)], \quad (1)$$

where \mathbf{w} is the model parameter, and $f(\mathbf{w}, \mathbf{x}_i)$ and $l(f(\mathbf{w}, \mathbf{x}_i), y_i)$ are the output of the network and the loss associated with a training example (\mathbf{x}_i, y_i) , respectively.

Spurious correlations and majority groups. Let \mathcal{S} be a set of *spurious* features that can be shared between classes. Examples in the dataset can be partitioned into different groups $g_{c,s}$, based on the combinations of their label and spurious feature (c, s) , where $c \in [\mathcal{C}]$, $s \in \mathcal{S}$. If a spurious feature s appears in majority of training examples of a class c , the group $g_{c,s}$ is called the *majority* group in class c . Other examples in class c are called *minority*. The ratio of majority group size to minority group size determines the degree of *spurious correlation* between spurious feature s and label c . Spurious features have a high correlation with a class in training data, resulting in poor test accuracy when encountering examples without the spurious features.

Fast- vs slow-learnable spurious feature. Fast-learnable features are those that learned early in training. These are typically features with little variation (e.g. only white balls), are simpler to learn and hence are typically learned by the network in early training epochs Nguyen et al. [2024]. In contrast, slow-learnable features are those learned later in training. These have higher variation (e.g. balls that can be any color) and consequently are more challenging to learn. Fast or slow-learnable spurious features, thus, refer to features that are spurious and learned either early or late in training.

Worst-group accuracy: Worst-group (WG) test accuracy refers to the lowest accuracy, at test time, across all groups $\mathcal{G} = \bigcup_{(c,s)} g_{c,s}$ Yang et al. [2024], Sagawa* et al. [2020], Creager et al. [2021], Liu et al. [2021]. Formally, WG test accuracy is defined as:

$$\text{WG} := \min_{g \in \mathcal{G}} \mathbb{E}_{(\mathbf{x}_i, y_i) \in g} [y_i = \hat{y}(\mathbf{w}, \mathbf{x}_i)],$$

where $\hat{y}(\mathbf{w}, \mathbf{x}_i)$ is the label predicted by the model.

Average accuracy: Average (AVG) test accuracy refers to a weighted average of test accuracy across groups, where the weight for each group is the fraction of examples in the training set from that group Yang et al. [2024], Sagawa* et al. [2020], Creager et al. [2021], Liu et al. [2021]. This quantifies the model performance on test data that i.i.d. to

the training data. Formally, AVG test accuracy is defined as:

$$\text{AVG} := \sum_{g \in \mathcal{G}} \frac{|g|}{|D|} \mathbb{E}_{(\mathbf{x}_i, y_i) \in g} [y_i = \hat{y}(\mathbf{w}, \mathbf{x}_i)],$$

where $\hat{y}(\mathbf{w}, \mathbf{x}_i)$ is the label predicted by the model.

Accuracy Disparity: Accuracy disparity typically refers to the phenomenon where different groups in the data encounter different accuracies Chi et al. [2021], Barocas et al. [2023]. Here, we quantify this disparity using the gap between WG and AVG accuracy. Formally, we define accuracy disparity as:

$$\text{DISPARITY} := \text{WG} - \text{AVG}.$$

4 EXPERIMENT DETAILS

Methods. We consider 8 SOTA methods aimed at improving worst-group accuracy affected by spurious correlations. We believe this is the first work to comprehensively evaluate SOTA methods specifically for this spurious correlations problem. Concretely, we cover the following algorithms in three categories: *vanilla*: **ERM** Vapnik [1991]; (1) *group inference methods*: **EIIL** Creager et al. [2021], **JTT** Liu et al. [2021], **SPARE** Yang et al. [2024]; (2) *validation group-known methods*: **SSA** Nam et al. [2022], **DFR** Kirichenko et al. [2023]; (3) *group-known robust methods*: **GB** Idrissi et al. [2022a], **GDRO** Sagawa* et al. [2020], **PDE** Deng* et al. [2023]. If group labels are available, group-known robust optimization (GDRO) Sagawa* et al. [2020] or up-sampling the minority groups Liu et al. [2021], Yang et al. [2024] can robustly train the model against spurious correlations, improving worst-group accuracy. Otherwise, group inference methods first infer groups within the training data based on a reference model trained with ERM, and then retrain the model using GDRO or sampling techniques with these inferred group labels. Validation group-known methods directly utilize the validation data to either infer the training groups or train the ERM model robustly. Appendix A provides a detailed descriptions for each method.

Model selection via validation set. Model selection (also known as hyperparameter tuning) is critical for all SOTA methods, much like in domain generalization approaches Gulrajani and Lopez-Paz [2020a]. Poor model selection, even from hyperparameter combinations from carefully chosen ranges, can lead to significant drops (over 70%) in worst-group test accuracy (see Sec. 7). To ensure fair evaluation, we extensively tune hyperparameters for these methods based on group-labeled validation data. Following Gulrajani and Lopez-Paz [2020b], Yang et al. [2023b], we randomly select 16 hyperparameter combinations from the grid, choose the top 3 combinations based on worst-group accuracy on the validation set, and re-run each with 3 different random seeds to report the best average result and its corresponding standard deviation. This procedure ensures

that our comparison is best-versus-best, with optimized hyperparameters for all algorithms. In total, we trained over 5K models.

5 FAST- & SLOW-LEARNABLE SPURIOUS FEATURES

We now study the effectiveness of existing methods in addressing fast and slow-learnable spurious features. Yang et al. [2024] demonstrated that models learn spurious correlations since spurious features are learned faster than true class features. Since a majority of each class can be classified correctly at training time using the spurious features, models do not learn the true class features and perform poorly on minority groups that lack the spurious features. To further investigate the impact of how quickly spurious features are learned on existing methods, we conduct a controlled study comparing fast and slow-learnable spurious features (both features are still learned faster than the true class feature so that models still learn the spurious correlations). Specifically, we introduce a new dataset SPUCoSUN, with a slow-learnable spurious feature and an alternate version, SPUCoSUN (Fast), which has a fast-learnable spurious feature. For both versions, since the spurious features are learned faster than the true class features, ERM exhibits very poor WG accuracy. Interestingly, our analysis reveals that spurious correlations arising from slow learnable spurious features are more challenging to mitigate for group inference methods. This highlights an open challenge for future group inference methods to address.

Table 1: Effect of Spurious Feature’s Difficulty: Larger accuracy disparity for group inference methods with slow-learnable spurious feature

	SPUCoSUN		SPUCoSUN (Fast)	
	WG	AVG	WG	AVG
ERM	29.3 \pm 1.4	96.0 \pm 0.2	21.9 \pm 3.51	96.7 \pm 0.1
JTT	55.8 \pm 1.1	88.8 \pm 0.6	63.5 \pm 0.3	85.1 \pm 0.4
SPARE	62.2 \pm 1.4	80.3 \pm 1.8	66.3 \pm 1.6	79.1 \pm 1.4
EIIL	65.9 \pm 1.3	76.1 \pm 3.1	64.4 \pm 3.2	79.0 \pm 4.2
SSA	68.7 \pm 0.8	83.9 \pm 0.8	66.0 \pm 0.6	79.4 \pm 4.9
DFR _{Tr} ^{Val}	67.3 \pm 1.6	79.9 \pm 2.6	68.2 \pm 0.7	80.1 \pm 1.5
GB	69.9 \pm 0.6	79.1 \pm 0.2	64.4 \pm 1.5	78.1 \pm 0.6
GDRO	65.5 \pm 2.3	78.2 \pm 0.8	64.7 \pm 1.8	77.4 \pm 4.8
PDE	67.6 \pm 0.8	77.7 \pm 1.2	66.0 \pm 2.7	77.4 \pm 0.3
		Slow-Learnable	Fast-Learnable	

5.1 DATASETS

SPUCoSUN (16 groups, 4 classes). SPUCoSUN is a dataset with 4 classes and 16 groups. The classes consist of

4 different types of backgrounds selected from the SUN397 dataset Xiao et al. [2010], namely {recreational, residential, cultural, infrastructure}. For each class, we generate spurious features as co-occurring objects, corresponding to categories from OpenImagesV7 Kuznetsova et al. [2020]. These co-occurring objects are generated using a text-to-image diffusion model Rombach et al. [2022]. The co-occurring objects for the aforementioned 4 classes are *sports equipment*, *fruits & vegetables*, *baked goods*, and *containers*, respectively. We use SPUCoSUN and SPUCoSUN (Fast) to refer to the versions with slow and fast learnable spurious features, respectively. For the slow-learnable spurious features, we sample three subcategories (from Kuznetsova et al. [2020]) to generate the spurious feature. Specifically, for sports equipment, we select basketball, golf ball, and tennis ball; for fruits & vegetables, we select pumpkin, watermelon, and broccoli; for baked goods, we select muffin, bagel, and pretzel; and for containers, we select waste container, can, and barrel. For the fast-learnable spurious features, we use only a single subcategory per spurious feature: sports equipment: golf ball, fruits & vegetables: watermelon, baked goods: bagel, and containers: barrel. There are 16 groups, specified by all the possible combinations of *class* (background) and *spurious* (co-occurring object) features. The majority groups are: 1) Recreational (BG) + Sports Equipment (CO Obj), 2) Residential (BG) + Fruits & Vegetables (CO Obj), 3) Cultural (BG) + Baked Goods (Co Obj) and 4) Infrastructure (BG) + Containers (Co Obj). The training set contains 28,092 examples per class, with the majority group comprising 98.5% of the examples, while each of the three minority groups accounts for 0.5%. The validation set has 1612 examples with balanced groups. The test set is group-balanced and has 4012 examples. Corresponding images in the two versions, SPUCoSUN and SPUCoSUN (Fast), are identical in all regards, except the spurious feature. Images from SPUCoSUN are shown in Fig. 6a. Figure 17 shows that the spurious feature of SPUCoSUN (Fast) is learned faster than the spurious feature of SPUCoSUN.

5.2 RESULTS AND ANALYSIS

Table 1 compares current SOTA methods across SPUCoSUN and SPUCoSUN (Fast), showing how different methods are affected by how quickly the spurious features are learned. Exact hyperparameters and experimental details appear in Appendix D.

Group-inference Methods Struggle in Presence of Slow-learnable Spurious Features. Fig. 4 compares the WG accuracy of ERM with the WG accuracy averaged across all Group Inference methods. While fast-learnable spurious features harm the WG accuracy of ERM more than slow-learnable spurious features, they are easier to address for Group Inference methods. Remarkably, when the spurious feature is learned quickly, the best Group Inference

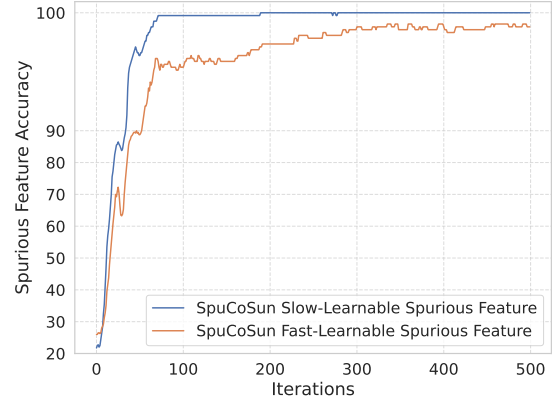


Figure 3: Comparing Average Accuracies of Majority and Minority Groups on SPUCoSUN (FAST) v/s SPUCoSUN

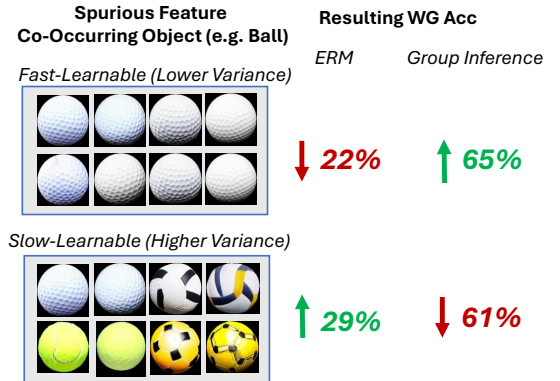


Figure 4: (Left) SPUCoSUN (Fast) v/s SPUCoSUN spurious feature, (Right) Both lead to poor WG accuracy with ERM, but group inference methods lag behind on improving WG Accuracy for slow-learnable spurious features

method (SPARE) performs comparably to the best method with group labels, PDE, in terms of both worst-group and average accuracy, as seen on SPUCoSUN (Fast). However, with slow-learnable spurious features, the performance of SPARE and JTT is significantly negatively impacted. Even EIIL, which appears as the best Group Inference method under more slowly learned spurious features and is relatively robust across the two datasets, falls far behind the performance of group-known methods like PDE on SPUCoSUN.

Inferred Group Membership is Less Accurate in the Presence of Slow-learnable Spurious Features. Models suffering from SC learn spurious features far faster than core features. Consequently, early in training, models rely almost *entirely on the spurious features for their predictions*. Group inference (GI) methods exploit this observation in various ways to infer groups. However, when the spurious feature cannot be learned as quickly, the model partially relies on core features for its predictions, even early in training. As a result, the underlying assumption behind existing GI methods breaks, and they can no longer infer groups

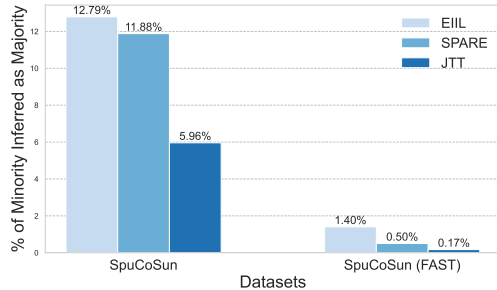


Figure 5: Large Fraction of Minority Inferred as Majority during Group Inference with Slow-Learnable Spurious Features

accurately. We confirm this in Fig. 5 by showing the fraction of minority group examples that GI methods misclassify as belonging to majority groups.

6 HIGHER NUMBER OF GROUPS & CLASSES

In this section, we study the effect of increasing the number of groups and classes on the effectiveness of existing methods in mitigating spurious correlations. We first present existing datasets and then introduce a new dataset with more classes and groups. It is important to note that conducting a controlled experiment in this context is fundamentally impossible, as altering the number of classes and groups necessarily changes other properties of the data (e.g., the learning speed of spurious or true class features). Nonetheless, our benchmarking of existing methods, across datasets with varying numbers of groups and classes, reveals trends that underscore the unsolved challenges posed by datasets with more groups and/or classes.

6.1 DATASETS & MODELS

We consider standard benchmark datasets for spurious correlations, namely Waterbirds and CelebA, both consisting of 2 classes and 4 groups. We also include the recently introduced UrbanCars dataset, which contains 2 classes and 8 groups. Additionally, we consider SPUCOSUN (described in Sec. 5.1), which has 4 classes and 16 groups. Furthermore, we introduce SPUCOANIMALS, a new dataset with 4 classes and 8 groups.

SpuCoAnimals (8 groups, 4 classes). SPUCOANIMALS is a large-scale vision dataset curated from ImageNet Deng et al. [2009] with 4 classes: {landbirds, waterbirds, small dogs, big dogs}, Waterbirds and landbirds are spuriously correlated with *water* (lake, river, sea) and, *land* (grass, forest and tree) backgrounds, respectively. Small dogs and big dogs are spuriously correlated with *indoor* (bed, couch and floor) and

outdoor (grass, park and road) backgrounds, respectively. The training set has 10500 examples per class with a 20:1 ratio between majority and minority group for each class. The validation set has 525 examples for each class with balanced groups. The test set has 500 examples per group. Fig. 6b shows examples of images from SPUCOANIMALS.

Model: CLIP-pretrained ResNet50. Prior work Liu et al. [2021], Creager et al. [2021], Yang et al. [2024], Kirichenko et al. [2023], Sagawa* et al. [2020] use an ImageNet pre-trained ResNet50 He et al. [2016] for group inference and robust training. To maintain consistency, we use the same setting for WATERBIRDS, CELEBA and URBANCARS. But, for all our datasets, we use a pretrained CLIP-ResNet50 to avoid potential data leakage from the ImageNet training set, as ImageNet-pretrained models may have already been trained on some of the images in our datasets.

6.2 RESULTS AND ANALYSIS




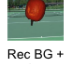
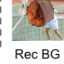
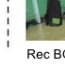
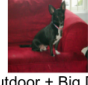

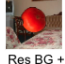
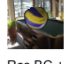
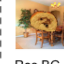
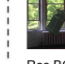






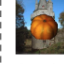







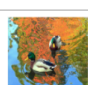
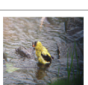
Table 3 shows the Worst-Group (WG) and Average (AVG) accuracy of all methods, on the above datasets.

Group-Balancing outperforms Group-DRO Interestingly, we find that across all datasets, simple Group-Balancing (GB) can achieve higher WG accuracy than the more sophisticated Group-DRO method. Group-DRO not only samples group-balanced batches during training but also computes a weighted loss over groups, assigning higher weights to worse-performing groups. The improvement of GB over Group-DRO is even more pronounced on datasets with more than 2 groups and/or more than 2 classes. This is likely due to the optimization challenges introduced by the frequent changes in the loss weights for different groups.

Accuracy Disparity is Larger with More Groups Figure 7 shows the accuracy disparity, i.e., the difference between WG and AVG accuracy, averaged across all methods for datasets with varying numbers of groups. We observe that the accuracy disparity increases almost linearly with the number of groups. This confirms that it becomes significantly more challenging for existing methods to reduce the accuracy disparity as the number of groups increases. Specifically, for WATERBIRDS and CELEBA, datasets with only 4 groups, the average accuracy disparity is relatively small, at no more than 5%. When the number of groups doubles to 8 in URBANCARS and SPUCOANIMALS, the accuracy disparity also doubles, reaching nearly 10%. Finally, on SPUCOSUN, which has 16 groups, the accuracy disparity is as high as 18%. Delving deeper into the results in Table 3, we see that even the best-performing method on each dataset struggles considerably as the number of groups increases. For example, the accuracy disparity for the best method, PDE, is less than 2.1% on datasets with 4 groups. However, as the number of groups increases from URBANCARS and SPUCOANIMALS to SPUCOSUN (Hard), the accuracy disparity for the best method rises to 7.9%, 8.6%, and 10.1%,

Table 2: Statistics of the six datasets used in our benchmark.

Dataset	Waterbirds	CelebA	UrbanCars	SpuCoAnimals	SpuCoSun (Hard)	SpuCoSun (Easy)
# Classes	2	2	2	4	4	4
# Groups	4	4	8	8	16	16
Train	4795	162770	7989	42000	28092	28092
Val.	1199	19867	999	2100	1612	1612
Test	5794	19962	1000	4000	4012	4012
Class Ratio	76.8:23.2	85:15	50:50	25:25:25:25	25:25:25:25	25:25:25:25
Train Maj.:Min.	95:5	52:48	94:6	95:5	98.5:0.5:0.5:0.5	98.5:0.5:0.5:0.5
Test Maj.:Min.	95:5	52:48	94:6	50:50	50:50	50:50

Spurious Features		Main Features	Majority Group (98.5%)	Minority Groups (Total size = 1.5%)			Majority Group (98.5%)	Minority Group (1.5%)
				0.5%	0.5%	0.5%		
ball 	fruit & veggie 	Recreational BG						
		Residential BG						
baked food 	containers 	Cultural BG						
		Infrastructure BG						

(a) SPUCOSUN

(b) SPUCOANIMALS

Figure 6: Construction and examples of images from our SPUCOSUN and SPUCOANIMALS datasets

Table 3: Effect of Number of Groups / Classes: WG & AVG accuracy (%) of training with SOTA algorithms. With more groups, accuracy disparity increases. With more classes, average accuracy is harder to maintain & there's a large spread in performance across methods

	WATERBIRDS		CELEBA		URBANCARS		SPUCOANIMALS		SPUCOSUN	
	WG	AVG	WG	AVG	WG	AVG	WG	AVG	WG	AVG
ERM	80.1 \pm 0.7	97.8 \pm 0.3	78.7 \pm 2.1	83.4 \pm 3.5	56.8 \pm 5.6	96.4 \pm 0.5	39.0 \pm 1.4	75.8 \pm 1.8	29.3 \pm 1.4	96.0 \pm 0.2
JTT	83.1 \pm 3.5	90.6 \pm 0.3	81.5 \pm 1.7	88.1 \pm 0.3	68.3 \pm 6.7	91.9 \pm 4.4	57.4 \pm 2.3	83.6 \pm 1.1	55.8 \pm 1.1	88.8 \pm 0.6
SPARE	91.6 \pm 0.8	96.2 \pm 0.6	86.5 \pm 3.3	89.8 \pm 0.3	80.5 \pm 3.9	90.3 \pm 2.5	61.6 \pm 2.4	76.5 \pm 1.1	62.2 \pm 1.4	80.3 \pm 1.8
EIIL	83.5 \pm 2.8	94.2 \pm 1.3	78.9 \pm 0.6	86.9 \pm 2.0	78.9 \pm 2.8	90.2 \pm 1.3	64.9 \pm 3.5	77.3 \pm 2.4	65.9 \pm 1.3	76.1 \pm 3.1
SSA	85.1 \pm 1.3	96.7 \pm 1.6	89.4 \pm 0.5	91.2 \pm 0.2	78.7 \pm 2.6	93.4 \pm 0.7	64.4 \pm 3.1	75.5 \pm 1.4	68.7 \pm 0.8	83.9 \pm 0.8
DFR _{Tr} ^{Val}	90.6 \pm 0.4	93.4 \pm 0.2	89.1 \pm 1.2	91.3 \pm 0.1	81.9 \pm 1.2	92.5 \pm 1.8	66.5 \pm 1.8	80.0 \pm 3.7	67.3 \pm 1.6	79.9 \pm 2.6
GB	88.1 \pm 0.6	95.5 \pm 0.4	88.6 \pm 1.0	91.1 \pm 0.1	82.7 \pm 2.0	92.8 \pm 0.0	69.9 \pm 0.1	79.1 \pm 0.1	69.9 \pm 0.6	79.1 \pm 0.2
GDRO	85.7 \pm 0.8	94.3 \pm 1.0	89.4 \pm 0.1	91.4 \pm 0.1	78.9 \pm 2.6	92.7 \pm 1.6	67.1 \pm 0.2	75.1 \pm 0.1	65.5 \pm 2.3	78.2 \pm 0.8
PDE	90.3 \pm 0.3	92.4 \pm 0.8	91.0 \pm 0.4	92.0 \pm 0.6	84.3 \pm 1.7	92.2 \pm 2.0	70.1 \pm 2.0	78.7 \pm 1.0	67.6 \pm 0.8	77.7 \pm 1.2

4 groups, 2 classes

8 groups, 2 classes

8 groups, 4 classes

16 groups, 4 classes

respectively. This increase in accuracy disparity is primarily caused by the difficulty of model selection—specifically, selecting optimal hyperparameters based on validation set WG accuracy—for datasets with more groups. As shown in Fig. 9, where we visualize the group-wise accuracy of simple Group Balancing on SPUCOSUN and WATERBIRDS,

datasets with more groups have a larger number of minority groups with lower accuracies. This makes it challenging to find a set of hyperparameters that optimizes performance across all poorly performing groups. Moreover, for robust training methods like GDRO, which weight losses for different groups based on their performance, the larger number of

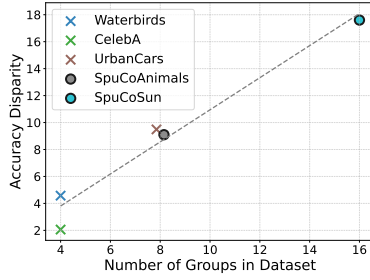


Figure 7: Accuracy disparity increases with # of groups

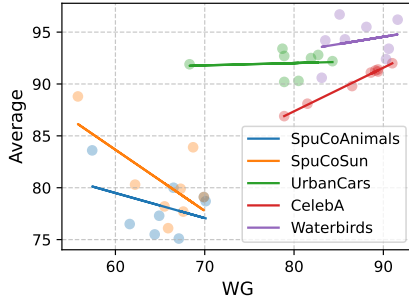


Figure 8: AVG vs. WG accuracy, averaged over different methods on each dataset. Waterbirds, CelebA, UrbanCars, SPUCOSUN and SPUCOANIMALS have 2, 2, 2, 4, 4 classes, respectively. As # classes increases more classes, improving WG accuracy more negatively affects AVG accuracy and the performance spread across methods widens.

groups further complicates optimization. Fig. 10 shows that the loss weights for different minority groups, even within the same class, vary significantly. This occurs despite all minority groups within a class having an equal number of samples. Notably, such imbalanced weighting among minority groups is not possible in datasets like WATERBIRDS and CELEBA, which have only a single minority group per class. This imbalance likely leads to overfitting to one of the minority groups rather than learning class features in a more generalizable manner. Addressing the larger accuracy disparity for datasets with more groups remains an unsolved challenge for methods tackling spurious correlations.

Maintaining a High Avg Acc when Data Has More Classes Is Difficult. Fig. 8 illustrates an interesting observation: when the data contains more classes, improving the worst-group (WG) accuracy negatively impacts the average (AVG) accuracy. Even when the number of groups is controlled (both URBANCARS and SPUCOANIMALS have 8 groups), increasing the number of classes (from 2 in URBANCARS to 4 in SPUCOANIMALS) shifts the correlation between WG and AVG accuracy from near zero to strongly negative, with a large spread in AVG accuracy across methods. Most state-of-the-art (SOTA) methods address spurious correlations (after group inference, if necessary) by upsampling identified minority group examples. The model then relies heavily on these upsampled examples to learn the

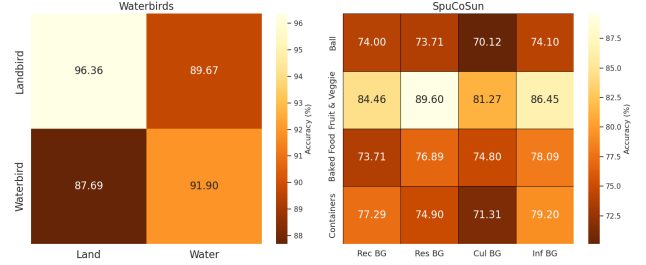


Figure 9: Heatmap of Group accuracies for Waterbirds and SPUCOSUN (Darker colors represent groups with lower accuracies)

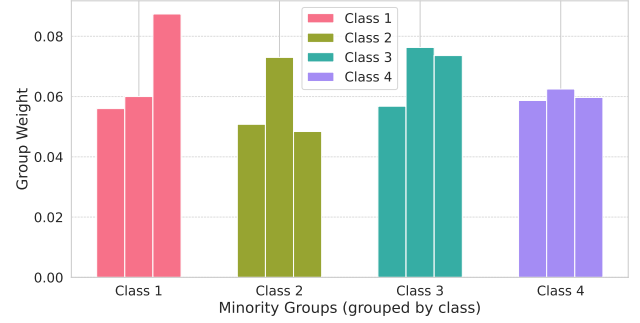


Figure 10: Group Weights for Minority Groups Computed by GroupDRO on SPUCOSUN (end of training)

true class feature. With more classes, as the classification problem becomes more challenging, it becomes increasingly critical to upsample examples with representative true class features, rather than outliers. The strong negative correlation and the large spread in AVG accuracy across methods (see Fig. 8) indicate that it is no longer sufficient to merely identify and upsample minority examples. Instead, it is essential to upsample minority examples that enable the model to generalizably learn the true class feature. This underscores a new challenge: maintaining high AVG accuracy while improving WG accuracy in the presence of more classes.

7 MODEL SELECTION

Model selection criteria determine which hyperparameters to use to obtain the best worst-group accuracy at test time. Gulrajani and Lopez-Paz [2020a] has studied and shown the importance of model selection criteria for domain generalization methods. We first make a similar observation for methods for spurious correlations and highlight how this is especially true with more groups and/or classes. Then, we demonstrate how effective model selection can help significantly when addressing multiple spurious features. After we have established the importance of model selection, we explore potential alternatives for reducing the high costs associated with model selection.

All Methods Are Highly Sensitive to Model Selection Fig. 11 shows the WG accuracy of the worst hyperparam-

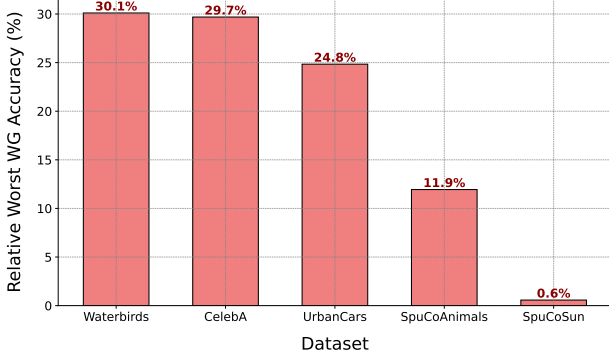


Figure 11: Normalized worst hyperparameter WG accuracy relative to best hyperparameter WG accuracy, averaged across methods and datasets. The low relative performance of the worst hyperparameters highlights the model’s high sensitivity to hyperparameter selection.

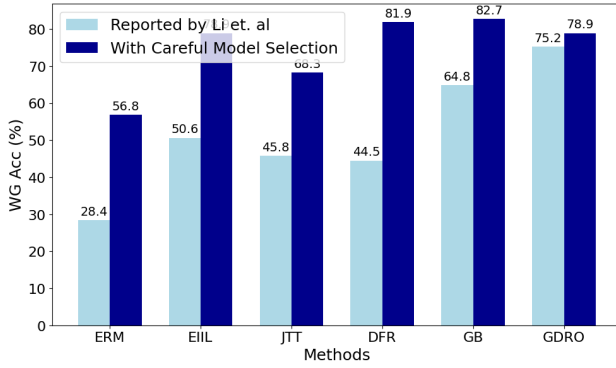


Figure 12: Showing Large Improvements on URBANCARS, Achieved through Careful Model Selection

eters, normalized by the WG accuracy of the best hyperparameters, across different datasets for all SOTA algorithms. For each method on existing datasets, we tuned based on the recommended hyperparameter ranges; for our datasets, we list our tuning ranges in Sec. E.2. We observe that across all datasets, the worst hyperparameter combinations within the recommended ranges achieve at most 30% of the WG accuracy of the best hyperparameters. The performance gap due to poor model selection is even more pronounced on datasets with more groups and/or classes (URBANCARS, SPUCOANIMALS, SPUCOSUN). Thus, a suboptimal choice of hyperparameters can significantly reduce method performance, necessitating thorough and costly model selection processes, which undermine the practicality of existing methods.

Model Selection in the Presence of Multiple Spurious Features Li et al. [2023] proposed URBANCARS, a dataset containing multiple spurious features, and highlighted the challenge of improving WG accuracy in this setting. They demonstrated that improving the performance of minority groups with respect to one spurious feature of-

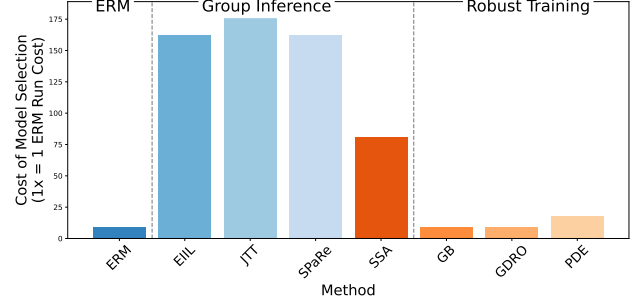


Figure 13: Highlighting the High Cost of Model Selection for Group Inference Methods

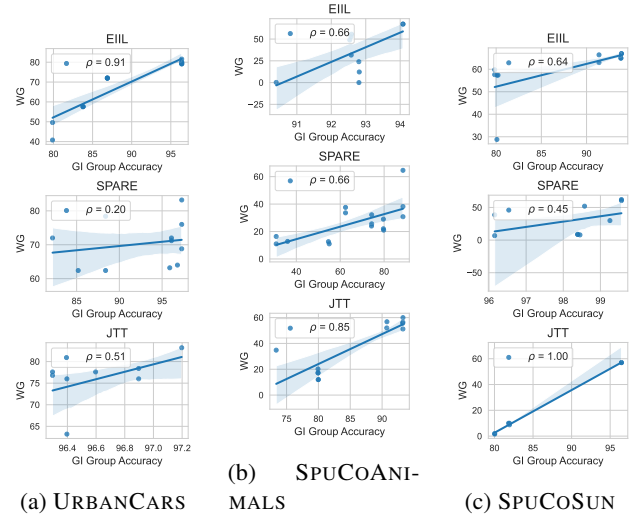


Figure 14: Positive Correlations between Accuracy of Inferred Groups and Resulting WG Accuracy

ten leads to a decrease in performance for minority groups corresponding to another spurious feature. Consequently, Li et al. [2023] observed consistently poor WG accuracy on URBANCARS across various methods. Here, we show that careful model selection can significantly mitigate this issue. For each method, we perform model selection by randomly sampling 16 hyperparameter combinations from the ranges specified for the respective method. Figure 12 compares the performance of SOTA algorithms as reported by Li et al. [2023] on URBANCARS with the results obtained through our model selection. Careful model selection achieves an average improvement of 23%, with gains as high as 37%.

Towards Efficient Model Selection for Group Inference Methods Fig. 13 shows that model selection is 100x more expensive for group inference methods, compared to others. This is due to the fact that for every potential combination of hyperparameters, these methods must infer groups, then train a model using the inferred groups, and then use the resulting validation worst-group accuracy as the model selection criterion. In many real-world scenarios, we do rely on these methods since group labels are not available

for training data and must be inferred. To remedy the very high costs of model selection for group inference methods, we investigate directly evaluating the quality of the inferred groups on the group-labeled validation set, by framing group inference as *majority* or *minority* as a classification problem (henceforth, referred to as *group inference accuracy*). Fig. 14 shows strong positive correlations of *group inference accuracy*, across group inference methods, with the final test worst-group accuracy. While these correlations are slightly weaker for SPARE, the trend remains consistent. Thus, we find that directly evaluating inferred groups is a promising approach for far more cost-efficient model selection for group inference methods.

8 CONCLUSION

We introduced three previously unexplored settings: 1) a larger number of classes, 2) a greater number of groups, and 3) slower-learned spurious features that pose challenges for existing methods aimed at improving worst-group (WG) accuracy in the presence of spurious features. Through extensive experiments, spanning 8 state-of-the-art (SOTA) methods and 5 datasets, we systematically evaluate the performance of these methods in mitigating spurious correlations under these new settings, uncovering several open challenges in this area. Additionally, we demonstrate that the optimal performance reported for SOTA methods is highly sensitive to model selection and propose an efficient alternative to the costly but crucial model selection process used in group inference methods. We hope our benchmark and findings will guide both theoreticians and practitioners in developing the next generation of methods to improve worst-group accuracy in the presence of spurious correlations.

Limitations. While our work introduced more challenging datasets and provided a comprehensive benchmark for evaluating SOTA methods addressing spurious correlations on vision tasks, generalizability of our findings to other domains, such as natural language processing, remains to be studied.

References

- Solon Barocas, Moritz Hardt, and Arvind Narayanan. *Fairness and machine learning: Limitations and opportunities*. MIT press, 2023.
- Jianfeng Chi, Yuan Tian, Geoffrey J Gordon, and Han Zhao. Understanding and mitigating accuracy disparity in regression. In *International conference on machine learning*, pages 1866–1876. PMLR, 2021.
- Elliot Creager, Jörn-Henrik Jacobsen, and Richard Zemel. Environment inference for invariant learning. In *International Conference on Machine Learning*, pages 2189–2200. PMLR, 2021.
- J. Deng, W. Dong, R. Socher, L.-J. Li, K. Li, and L. Fei-Fei. ImageNet: A Large-Scale Hierarchical Image Database. In *CVPR09*, 2009.
- Yihe Deng*, Yu Yang*, Baharan Mirzasoleiman, and Quanquan Gu. Robust learning with progressive data expansion against spurious correlation. In A. Oh, T. Naumann, A. Globerson, K. Saenko, M. Hardt, and S. Levine, editors, *Advances in Neural Information Processing Systems*, volume 36, pages 1390–1402. Curran Associates, Inc., 2023. URL https://proceedings.neurips.cc/paper_files/paper/2023/file/0506ad3d1bcc8398a920db9340f27fe4-Paper-Conference.pdf.
- Ishaan Gulrajani and David Lopez-Paz. In search of lost domain generalization, 2020a.
- Ishaan Gulrajani and David Lopez-Paz. In search of lost domain generalization. *arXiv preprint arXiv:2007.01434*, 2020b.
- Kaiming He, Xiangyu Zhang, Shaoqing Ren, and Jian Sun. Deep residual learning for image recognition. In *Proceedings of the IEEE conference on computer vision and pattern recognition*, pages 770–778, 2016.
- Yue He, Zheyang Shen, and Peng Cui. Towards non-iid image classification: A dataset and baselines. *Pattern Recognition*, 110:107383, 2021.
- Dan Hendrycks, Steven Basart, Norman Mu, Saurav Kadavath, Frank Wang, Evan Dorundo, Rahul Desai, Tyler Zhu, Samyak Parajuli, Mike Guo, et al. The many faces of robustness: A critical analysis of out-of-distribution generalization. In *Proceedings of the IEEE/CVF international conference on computer vision*, pages 8340–8349, 2021a.
- Dan Hendrycks, Kevin Zhao, Steven Basart, Jacob Steinhardt, and Dawn Song. Natural adversarial examples. In *Proceedings of the IEEE/CVF conference on computer vision and pattern recognition*, pages 15262–15271, 2021b.
- Badr Youbi Idrissi, Martin Arjovsky, Mohammad Pezeshki, and David Lopez-Paz. Simple data balancing achieves competitive worst-group-accuracy, 2022a.
- Badr Youbi Idrissi, Diane Bouchacourt, Randall Balestriero, Ivan Evtimov, Caner Hazirbas, Nicolas Ballas, Pascal Vincent, Michal Drozdal, David Lopez-Paz, and Mark Ibrahim. Imagenet-x: Understanding model mistakes with factor of variation annotations. *arXiv preprint arXiv:2211.01866*, 2022b.
- Eunyeup Kim, Jiyeon Lee, and Jaegul Choo. Biaswap: Removing dataset bias with bias-tailored swapping augmentation, 2021.
- Polina Kirichenko, Pavel Izmailov, and Andrew Gordon Wilson. Last layer re-training is sufficient for robustness to spurious correlations. In *The Eleventh International Conference on Learning Representations*, 2023. URL <https://openreview.net/forum?id=Zb6c8A-Fghk>.
- Alexander Kirillov, Eric Mintun, Nikhila Ravi, Hanzi Mao, Chloe Rolland, Laura Gustafson, Tete Xiao, Spencer Whitehead, Alexander C. Berg, Wan-Yen Lo, Piotr Dollár, and Ross Girshick. Segment anything. *arXiv:2304.02643*, 2023.

- Pang Wei Koh, Shiori Sagawa, Henrik Marklund, Sang Michael Xie, Marvin Zhang, Akshay Balsubramani, Weihua Hu, Michihiro Yasunaga, Richard Lanus Phillips, Irena Gao, Tony Lee, Etienne David, Ian Stavness, Wei Guo, Berton A. Earnshaw, Imran S. Haque, Sara Beery, Jure Leskovec, Anshul Kundaje, Emma Pierson, Sergey Levine, Chelsea Finn, and Percy Liang. Wilds: A benchmark of in-the-wild distribution shifts, 2021.
- Alina Kuznetsova, Hassan Rom, Neil Alldrin, Jasper Uijlings, Ivan Krasin, Jordi Pont-Tuset, Shahab Kamali, Stefan Popov, Matteo Mallocci, Alexander Kolesnikov, Tom Duerig, and Vittorio Ferrari. The open images dataset v4: Unified image classification, object detection, and visual relationship detection at scale. *IJCV*, 2020.
- Zhiheng Li, Ivan Evtimov, Albert Gordo, Caner Hazirbas, Tal Hassner, Cristian Canton Ferrer, Chenliang Xu, and Mark Ibrahim. A whac-a-mole dilemma: Shortcuts come in multiples where mitigating one amplifies others. In *Proceedings of the IEEE/CVF Conference on Computer Vision and Pattern Recognition (CVPR)*, pages 20071–20082, June 2023.
- Evan Z Liu, Behzad Haghighi, Annie S Chen, Aditi Raghunathan, Pang Wei Koh, Shiori Sagawa, Percy Liang, and Chelsea Finn. Just train twice: Improving group robustness without training group information. In *International Conference on Machine Learning*, pages 6781–6792. PMLR, 2021.
- Ziwei Liu, Ping Luo, Xiaogang Wang, and Xiaoou Tang. Deep learning face attributes in the wild. In *Proceedings of International Conference on Computer Vision (ICCV)*, December 2015.
- David Madras and Richard Zemel. Identifying and benchmarking natural out-of-context prediction problems. *Advances in Neural Information Processing Systems*, 34:15344–15358, 2021.
- Junhyun Nam, Hyuntak Cha, Sungsoo Ahn, Jaeho Lee, and Jinwoo Shin. Learning from failure: Training debiased classifier from biased classifier. In *Advances in Neural Information Processing Systems*, 2020.
- Junhyun Nam, Jaehyung Kim, Jaeho Lee, and Jinwoo Shin. Spread spurious attribute: Improving worst-group accuracy with spurious attribute estimation. In *International Conference on Learning Representations*, 2022. URL https://openreview.net/forum?id=_F9xpOrqyX9.
- Dang Nguyen, Paymon Haddad, Eric Gan, and Baharan Mirza-soleiman. Make the most of your data: Changing the training data distribution to improve in-distribution generalization performance. *arXiv preprint arXiv:2404.17768*, 2024.
- Alec Radford, Jong Wook Kim, Chris Hallacy, Aditya Ramesh, Gabriel Goh, Sandhini Agarwal, Girish Sastry, Amanda Askell, Pamela Mishkin, Jack Clark, Gretchen Krueger, and Ilya Sutskever. Learning transferable visual models from natural language supervision, 2021.
- Robin Rombach, Andreas Blattmann, Dominik Lorenz, Patrick Esser, and Björn Ommer. High-resolution image synthesis with latent diffusion models. In *Proceedings of the IEEE/CVF Conference on Computer Vision and Pattern Recognition (CVPR)*, pages 10684–10695, June 2022.
- Shiori Sagawa*, Pang Wei Koh*, Tatsunori B. Hashimoto, and Percy Liang. Distributionally robust neural networks. In *International Conference on Learning Representations*, 2020. URL <https://openreview.net/forum?id=ryxGuJrFvS>.
- Rohan Taori, Achal Dave, Vaishal Shankar, Nicholas Carlini, Benjamin Recht, and Ludwig Schmidt. Measuring robustness to natural distribution shifts in image classification. *Advances in Neural Information Processing Systems*, 33:18583–18599, 2020.
- Vladimir Vapnik. Principles of risk minimization for learning theory. *Advances in neural information processing systems*, 4, 1991.
- Jianxiong Xiao, James Hays, Krista A. Ehinger, Aude Oliva, and Antonio Torralba. Sun database: Large-scale scene recognition from abbey to zoo. In *2010 IEEE Computer Society Conference on Computer Vision and Pattern Recognition*, pages 3485–3492, 2010. doi: 10.1109/CVPR.2010.5539970.
- Yu Yang, Besmira Nushi, Hamid Palangi, and Baharan Mirza-soleiman. Mitigating spurious correlations in multi-modal models during fine-tuning. In Andreas Krause, Emma Brunskill, Kyunghyun Cho, Barbara Engelhardt, Sivan Sabato, and Jonathan Scarlett, editors, *Proceedings of the 40th International Conference on Machine Learning*, volume 202 of *Proceedings of Machine Learning Research*, pages 39365–39379. PMLR, 23–29 Jul 2023a. URL <https://proceedings.mlr.press/v202/yang23j.html>.
- Yu Yang, Eric Gan, Gintare Karolina Dziugaite, and Baharan Mirza-soleiman. Identifying spurious biases early in training through the lens of simplicity bias. In Sanjoy Dasgupta, Stephan Mandt, and Yingzhen Li, editors, *Proceedings of The 27th International Conference on Artificial Intelligence and Statistics*, volume 238 of *Proceedings of Machine Learning Research*, pages 2953–2961. PMLR, 02–04 May 2024. URL <https://proceedings.mlr.press/v238/yang24c.html>.
- Yuzhe Yang, Haoran Zhang, Dina Katabi, and Marzyeh Ghassemi. Change is hard: A closer look at subpopulation shift, 2023b.
- Xingxuan Zhang, Yue He, Renzhe Xu, Han Yu, Zheyang Shen, and Peng Cui. Nico++: Towards better benchmarking for domain generalization. In *Proceedings of the IEEE/CVF Conference on Computer Vision and Pattern Recognition*, pages 16036–16047, 2023.

A EXISTING METHODS

Several methods have been proposed to prevent models from exploiting spurious correlations and improve worst group error. If group labels are available, group robust optimization or sampling methods upweight or upsample the minority groups to achieve a similar accuracy on all groups. If group labels are not available, existing methods first infer groups of the training data and then train the model using robust optimization or sampling techniques with the inferred group labels.

A.1 WITH GROUP LABELED TRAINING DATA

Group Balancing samples every mini-batch to have equal examples from each group.

GroupDRO (GDRO) leverages group information to sample group-balanced batches of training data, and minimizes the empirical worst-group training loss:

$$\mathbf{w} \in \arg \min \max_{g \in \mathcal{G}} \mathbb{E}_{(\mathbf{x}_i, y_i) \in g} [l(f(\mathbf{w}, \mathbf{x}_i), y_i)]. \quad (2)$$

GroupDRO solves the above optimization problem by maintaining a weight q_g for each group g and weighting the loss of examples in group g by q_g . Stochastic gradient descent on parameter \mathbf{w} is interleaved with gradient ascent on the weights q_g . GDRO uses a very small tunable learning rate and a large regularizer to achieve a satisfactory performance.

PDE is a two-stage training algorithm designed to mitigate spurious correlations by progressively expanding the training data. In the warm-up stage, a small, balanced subset of data is used to prevent the model from learning spurious features. In the expansion stage, small random subsets of the remaining data are incrementally added, leveraging the momentum from the warm-up stage to continue learning core features effectively.

A.2 WITHOUT GROUP LABELED DATA

In absence of group labels, methods typically infer groups, often using a reference model f_{ref} trained with ERM, and then leverage the inferred groups to train a robust model using sampling or GDRO.

Just Train Twice (JTT) Liu et al. [2021] first trains a reference model f_{ref} using ERM for T_r number of epochs. Then, it identifies the minority group as examples that are misclassified by the reference model. JTT then upsamples the misclassified examples S_r times and trains another model using ERM on the upsampled dataset. T_r and S_r are tuned to achieve the optimal performance.

Environment Inference for Invariant Learning (EIIL) EIIL consists of two stages: environment (Group) inference (EI) and invariant learning (IL). In the EI stage, EIIL aims to infer the worst-case groups (environments) using a reference model f_{ref} that has been trained with ERM by optimizing a soft-group assignment \mathbf{q} to maximize the following objective:

$$C^{EI}(f_{ref}, \mathbf{q}) = \|\nabla_{\bar{\mathbf{w}}} \tilde{R}^e(\bar{\mathbf{w}} \cdot f_{ref}, \mathbf{q})\|. \quad (3)$$

$$\text{s.t. } \tilde{R}^e(f_{ref}, \mathbf{q}) = \frac{1}{N} \sum_i q_i(e) l(f_{ref}(\mathbf{x}_i), y_i). \quad (4)$$

where $\bar{\mathbf{w}}$ is the all-ones vector. Intuitively, the group assignment \mathbf{q} is optimized to find examples that are most sensitive to small changes in the reference model f_{ref} 's outputs. In the IL stage, EIIL uses GroupDRO with the inferred groups to train a robust model.

Separate Early and Re-sample (SPARE) SPARE Yang et al. [2024] proved that in the presence of strong spurious correlations, the outputs of a neural network trained with ERM are mainly determined by the spurious features, early-in-training. Thus, it infers groups by clustering the reference model f_{ref} 's output on each class, where f_{ref} is trained for a few T_r epochs. The inferred groups (clusters) are then used to train a model with importance sampling based on the cluster sizes, to balance the groups. Number of clusters and T_r are tuned to achieve best performance.

A.3 USING THE GROUP-LABELED VALIDATION SET

Spread Spurious Attributes (SSA) SSA [Nam et al., 2022] leverages the group labeled validation data to train a group label predictor in a semi-supervised manner. Given a training example \mathbf{x}_i , let g denotes its (unknown) group label, $\hat{p}(\cdot | \mathbf{x}_i)$

denotes the model’s predicted group label distribution and $\hat{g} := \arg \max_{g \in \mathcal{A}} \hat{p}(g|\mathbf{x}_i)$ denotes the predicted group label. SSA minimizes the following loss function:

$$\begin{aligned} \mathcal{L} = & \hat{\mathbb{E}}_{\text{group labeled}} [\text{CE}(\hat{p}(\cdot|\mathbf{x}), g)] \\ & + \hat{\mathbb{E}}_{\text{group-unlabeled}} [\mathbb{1}_{\max_{g \in \mathcal{A}} \hat{p}(g|\mathbf{x}) \geq \tau} \text{CE}(\hat{p}(\cdot|\mathbf{x}), \hat{g})], \end{aligned} \quad (5)$$

where CE is the cross entropy loss. Effectively, in addition to fitting the available group labels (validation set), SSA uses the group unlabeled examples with confident predictions (larger than a threshold τ) as additional group labeled data. Moreover, SSA partitions the group unlabeled data into multiple splits and trains a group label predictor for each left-out split by using the other splits as the group unlabeled training data. The threshold τ and the number of splits are both tuned to achieve optimal performance.

Deep Feature Reweighting (DFR) DFR Kirichenko et al. [2023] argues that a model trained with ERM captures both core and spurious features in its last hidden layer, even though it may exhibit spurious correlations in its predictions. Motivated by this, DFR retrains the last linear layer of the model on a group-balanced validation data, while keeping earlier layers frozen. This enables the model to adjust the weights assigned to the features in the penultimate layer. DFR trains multiple linear models with tunable ℓ_1 regularization on randomly sampled group-balanced validation data and averages their weights.

B SPUCOANIMALS DETAILS

B.1 DATASET DETAILS

B.1.1 Grouping of Fine-Grained ImageNet Classes for SpuCoAnimals Classes

Landbirds and Waterbirds. Landbirds are birds that primarily inhabit terrestrial environments, while waterbirds are birds that primarily inhabit aquatic or semi-aquatic habitats. This is identical to the grouping of birds used by Waterbirds Sagawa* et al. [2020].

```
landbirds = [rooster, hen, ostrich, brambling, goldfinch, house finch, junco,
indigo bunting, American robin, bulbul, jay, magpie, chickadee, American
dipper, kite (bird of prey), bald eagle, vulture, great grey owl, black grouse,
ptarmigan, ruffed grouse, prairie grouse, peafowl, quail, partridge, african grey
parrot, macaw, sulphur-crested cockatoo, lorikeet, coucal, bee eater, hornbill,
hummingbird, jacamar, toucan]
```

```
waterbirds = [duck, red-breasted merganser, goose, black swan, white stork, black
stork, spoonbill, flamingo, little blue heron, great egret, bittern bird, crane
bird, limpkin, common gallinule, American coot, bustard, ruddy turnstone, dunlin,
common redshank, dowitcher, oystercatcher, pelican, king penguin, albatross]
```

Small Dogs and Big Dogs. The two lists of dogs correspond to categorization based on their respective sizes. The first list consists of small dog breeds commonly referred to as "toy" or "toy terrier" breeds. These dogs are typically small in size and often kept as companion pets. Examples include Chihuahua, Maltese, Shih Tzu, and Yorkshire Terrier. The second list consists of a variety of dog breeds, including medium-sized and large-sized breeds. These breeds are specifically not classified as toy breeds. Examples from this list include Labrador Retriever, German Shepherd Dog, Rottweiler, Great Dane, Alaskan Malamute, and Siberian Husky. These breeds are often known for their working abilities, guarding skills, or other specific purposes.

```
small dog breeds = [Chihuahua, Japanese Chin, Maltese, Pekingese, Shih Tzu, King
Charles Spaniel, Papillon, toy terrier, Italian Greyhound, Whippet, Ibizan Hound,
Norwegian Elkhound, Yorkshire Terrier, Norfolk Terrier, Norwich Terrier, Wire Fox
Terrier, Lakeland Terrier, Sealyham Terrier, Cairn Terrier, Australian Terrier,
Dandie Dinmont Terrier, Boston Terrier, Miniature Schnauzer, Scottish Terrier,
Tibetan Terrier, Australian Silky Terrier, West Highland White Terrier, Lhasa
Apso, Soft-coated Wheaten Terrier, Australian Kelpie, Shetland Sheepdog, Pembroke
Welsh Corgi, Cardigan Welsh Corgi, Toy Poodle, Miniature Poodle, Mexican hairless
dog (xoloitzcuintli)]
```

```
big dog breeds = [Rhodesian Ridgeback, Afghan Hound, Basset Hound, Beagle,
Bloodhound, Bluetick Coonhound, Black and Tan Coonhound, Treeing Walker
Coonhound, English foxhound, Redbone Coonhound, borzoi, Irish Wolfhound,
Otterhound, Saluki, Scottish Deerhound, Weimaraner, Staffordshire Bull Terrier,
American Staffordshire Terrier, Bedlington Terrier, Border Terrier, Kerry Blue
Terrier, Irish Terrier, Flat-Coated Retriever, Curly-coated Retriever, Golden
Retriever, Labrador Retriever, Chesapeake Bay Retriever, German Shorthaired
Pointer, Vizsla, English Setter, Irish Setter, Gordon Setter, Brittany dog,
Clumber Spaniel, English Springer Spaniel, Welsh Springer Spaniel, Cocker
Spaniel, Sussex Spaniel, Irish Water Spaniel, Kuvasz, Schipperke, Groenendael
dog, Malinois, Briard, Komondor, Old English Sheepdog, collie, Border Collie,
Bouvier des Flandres dog, Rottweiler, German Shepherd Dog, Doberman, Greater
Swiss Mountain Dog, Bernese Mountain Dog, Appenzeller Sennenhund, Entlebucher
Sennenhund, Boxer, Bullmastiff, Tibetan Mastiff, French Bulldog, Great Dane, St.
Bernard, Alaskan Malamute, Siberian Husky, Leonberger, Newfoundland dog, Great
Pyrenees dog, Samoyed, Chow Chow, Keeshond, Dalmatian, Affenpinscher, Basenji,
pug]
```

B.1.2 Statistics about Data

Table 4: Number of Examples per Group in Train, Validation and Test Sets of SPUCoANIMALS

Data Split	Landbirds		Waterbirds		Small Dogs		Big Dogs	
	Land	Water	Land	Water	Indoor	Outdoor	Indoor	Outdoor
Train	10000	500	500	10000	10000	500	500	10000
Validation	500	25	25	500	500	25	25	500
Test	500	500	500	500	500	500	500	500

Variety in Spurious Features

Here, we show how many examples for each spurious environment correspond to each of the prompts used to identify the environments. This illustrates the diversity in spurious features in SpuCoAnimals, which as shown in Yang et al. [2023b] determines the effectiveness of methods to improve worst-group accuracy.

For spurious feature = “outdoor”: Big Dog Outdoor: (grass, 9222), (park, 734), (road, 44) Small Dog Outdoor: (grass, 472), (park, 25), (road, 3)

For spurious feature = “indoor”: Big Dog Indoor: (couch, 5408), (floor, 3252), (bed, 1340) Small Dog Indoor: (couch, 266), (floor, 196), (bed, 38)

For spurious feature = “land”: Landbirds Land: (grass, 7441), (tree, 1395), (tree, 1164) Waterbirds Land: (grass, 469), (forest, 18), (tree, 13)

For spurious feature = “water”: Landbirds Water: (river, 218), (sea, 179), (lake, 103) Waterbirds Water: (lake, 5367), (sea, 3640), (river, 989), (ocean, 4)

Table 5: Accuracy on each group for models trained and evaluated on the modified versions of SPUCOSUN where no spurious correlation exists. The model is trained using ERM. Here, Group ID is in the format of (Class ID, Spurious Attribute ID).

Group ID	Masked-Spurious	Core-Only
(0, 0)	73.6	82.8
(0, 1)	73.3	84.1
(0, 2)	71.3	85.3
(0, 3)	72.1	83.7
(1, 0)	76.5	92.4
(1, 1)	82.0	94.4
(1, 2)	72.1	88.5
(1, 3)	76.1	92.8
(2, 0)	75.7	84.5
(2, 1)	76.5	86.5
(2, 2)	76.4	83.6
(2, 3)	73.7	85.7
(3, 0)	76.9	87.3
(3, 1)	79.7	84.9
(3, 2)	75.7	87.6
(3, 3)	83.2	84.8

B.1.3 Examples

Fig. 15 and Fig. 16 show examples from each group of examples from birds and dogs respectively.

B.2 ABLATIONS ON SPUCOSUN

To demonstrate the learnability of the core feature on SPUCOSUN, we construct two additional versions of the dataset where no spurious correlation exists: (1) Masked-Spurious, where we mask out the spurious features, and (2) Core-Only, where we do not add the spurious feature to the core, e.g., just the corresponding original image from the SUN397 dataset. The accuracy achieved by ERM on these modified datasets should serve as the upper bound for our target performance, as this represents the scenario where no spurious correlation issues are present. In Table 5, we show the per-group accuracy achieved by ERM on both datasets. We see that the worst-group accuracy here is higher than those presented for SPUCOSUN in Table 3, indicating significant room for improvement for existing methods, including those with known group information.

C SPUCOSUN

C.1 CONSTRUCTION OF SPUCOSUN

The SPUCOSUN dataset was constructed through a series of steps to ensure a diverse and challenging dataset for machine learning experiments. Below are the detailed steps involved in its creation:

1. Selection of Superclasses from SUN397:

- Four superclasses were chosen from the SUN397 dataset: Recreational, Residential, Cultural, and Infrastructure.
- These superclasses formed the basis for the classes in the SPUCOSUN dataset.

2. Incorporation of Spurious Features:

- To add spurious features, we introduced co-occurring objects from the OpenImagesV7 dataset.
- The chosen objects were from specific categories: sports equipment (basketball, golf ball, tennis ball), fruits & vegetables (pumpkin, watermelon, broccoli), baked goods (muffin, bagel, pretzel), and containers (waste container, can, barrel).

3. Variation in Spurious Features:

- For SPUCOSUN (Fast), the spurious co-occurring object was sampled from only one subclass.
- For SPUCOSUN, the spurious feature’s variation was increased by sampling the spurious co-occurring object from all three subclasses, making the learning task more challenging.

4. Generation of Co-occurring Objects:

- We used a Text-To-Image Latent Diffusion Model Rombach et al. [2022] to generate the co-occurring objects.
- The prompt used for generating these objects was "*a **classname** on black background*".

5. Image Resizing:

- The background image, representing the class feature, was resized to (224,224) pixels.
- This resizing was done for all selected images from SUN397.

6. Segmentation of Co-occurring Objects:

- The SegmentAnythingModel Kirillov et al. [2023] was utilized to obtain a fine-grained mask of the co-occurring object generated by the diffusion model.

7. Resizing Co-occurring Objects:

- The segmented co-occurring object was resized, preserving its aspect ratio, to fit within the central (112,112) pixels of the (224,224) background image.

8. Validation of Dataset without Spurious Features:

- To confirm that the spurious feature’s masking does not render the class unlearnable, we created a version of the dataset without the spurious feature.
- In this version, the central (112,112) pixels were masked out, and a CLIP pre-trained ResNet-50 model was trained with ERM on this modified dataset.
- The model achieved an accuracy of 76.8%, indicating that the task remains solvable even with the spurious feature occlusion.

These steps collectively ensured the SPUCOSUN dataset was robust and suitable for evaluating the influence of spurious features in machine learning tasks.

C.2 EMPIRICALLY CONFIRMING THAT SPURIOUS FEATURE OF SPUCOSUN (FAST) IS EASIER THAN THAT OF SPUCOSUN

Figure 17 shows that the spurious feature of SPUCOSUN (Fast) is learned faster than the spurious feature of SPUCOSUN.

D OPTIMAL HYPERPARAMETERS (USED FOR RESULTS REPORTED IN TABLE 3 AND 1)

In this section, we present the optimal hyperparameters found via our model selection to report the results in Table 3. For existing datasets i.e. WATERBIRDS, CELEBA, URBANCARS, we follow previous work and use a ResNet-50, pre-trained on ImageNet. For the new datasets proposed in this work i.e. SPUCOANIMALS, SPUCOSUN (Easy) and SPUCOSUN (Hard), we use a ResNet-50, pretrained with CLIP Radford et al. [2021] and only train the final projection layer as in Yang et al. [2023a]. For all experiments, we use batch size of 128 as is standard on previous datasets.

Table 6: Number of Epochs for Robust Training on Each Dataset

	WATERBIRDS	CELEBA	URBANCARS
Epochs	300	50	300
	SPUCOANIMALS	SPUCOSUN (Hard)	SPUCOSUN (Easy)
Epochs	100	40	40

Table 7: SPARE

	WATERBIRDS	CELEBA	URBANCARS
LR	1e-3	1e-5	1e-4
WD	1e-4	1e-0	1e-1
Infer epoch	2	1	1
N clusters	2	2	4
Upsample power	3	2	2
	SPUCOANIMALS	SPUCOSUN (Hard)	SPUCOSUN (Easy)
LR	1e-4	1e-3	1e-4
WD	1e-2	1e-2	1e-1
Infer epoch	2	1	2
N clusters	2	4	4
Upsample power	2	2	1

Table 8: PDE

	WATERBIRDS	CELEBA	URBANCARS
LR	1e-2	1e-2	1e-3
WD	1e-2	1e-4	1e-1
Warmup length	140	16	75
Expand size	10	50	10
Expand interval	10	10	30
Subsample min	-	-	150
	SPUCOANIMALS	SPUCOSUN (Hard)	SPUCOSUN (Easy)
LR	1e-3	1e-2	1e-2
WD	1e-3	1e-4	1e-3
Warmup length	20	20	20
Expand size	10	50	10
Expand interval	2	2	2
Subsample min	-	-	-

Table 9: ERM

	WATERBIRDS	CELEBA	URBANCARS
LR	1e-3	1e-4	1e-4
WD	1e-4	1e-1	1e-1
	SPUCoANIMALS	SPUCoSUN (Hard)	SPUCoSUN (Easy)
LR	1e-3	1e-5	1e-5
WD	1e-4	1e-4	1e-4

Table 10: GDRO

	WATERBIRDS	CELEBA	URBANCARS
LR	1e-5	1e-4	1e-4
WD	1	1	1
	SPUCoANIMALS	SPUCoSUN (Hard)	SPUCoSUN (Easy)
LR	1e-5	1e-5	1e-5
WD	1e-4	1	1

E MODEL SELECTION

E.1 GROUP INFERENCE EVALUATION METRICS

For the group inference metrics, we consider each class as having two groups: 1) examples that have the spurious feature correlated with this class in the training data (the majority group in the training data, henceforth referred to as the *majority* group), and 2) examples that do not have the spurious feature correlated with this class in the training data (the minority group(s) in the training data, henceforth referred to as the *minority* group).

Note that in datasets such as SPUCoSUN and URBANCARS, there are multiple *groups* that do not have the spurious feature correlated with the class. In these cases, the *minority* group refers to the union of all these groups.

Having defined two groups per class, we evaluate group inference metrics by assessing how often they correctly identify whether an example belongs to the *majority* group or the *minority* group. Here, belonging to the *minority* group is considered the positive label, and precision and recall are defined with respect to this label.

Since we evaluate accuracy, precision, and recall per class, our analysis includes both average precision/recall and minimum precision/recall per class. For accuracy, we only report the overall accuracy across all classes, rather than considering minimum accuracy.

We now go into specific details about how we compute group inference metrics for each method considered in this paper. Our approach is general and can be applied to any group inference method.

JTT For JTT, we classify the examples of the validation set, and those misclassified are determined as the error set. We treat this as the *minority* group and the rest as the *majority* group. We then partition these groups using the provided class labels, allowing us to evaluate our group inference metrics.

EIIL For EIIL, we run the group inference algorithm on the validation set. Since the groups are symmetric for EIIL, on a group-balanced validation set, either group could be the *majority* or *minority*. Therefore, we assign the *majority* and *minority* labels to both groups and select the assignment with the higher accuracy to ensure our labeling is correct. We then use this assignment to compute the accuracy, recall, and precision metrics.

SPARE For SPARE, we run the clustering algorithm on the validation set to determine validation set groups. Similar to EIIL, on a group-balanced validation set, any of the groups could correspond to the *majority*. Therefore, we first consider each group of a class as the *majority*, then merge all other groups into the *minority* and evaluate accuracy. We select the *majority* assignment that achieves the highest accuracy. This process is repeated for each class since SPARE infers groups per class. We then use this assignment to compute the accuracy, recall, and precision metrics.

Table 11: GB

	WATERBIRDS	CELEBA	URBANCARS
LR	1e-5	1e-4	1e-4
WD	1	1	1
	SPUCOANIMALS	SPUCOSUN (Hard)	SPUCOSUN (Easy)
LR	1e-5	1e-5	1e-5
WD	1e-4	1	1

Table 12: JTT

	WATERBIRDS	CELEBA	URBANCARS
LR	1e-5	1e-5	1e-4
WD	1	1e-1	1e-1
Infer epoch	60	1	2
Upsampling Power	100	50	50
	SPUCOANIMALS	SPUCOSUN (Hard)	SPUCOSUN (Easy)
LR	1e-3	1e-3	1e-3
WD		1e-5	1e-5
Infer epoch	1	1	2
Upsampling Power	100	100	100

E.2 HYPERPARAMETER RANGES FOR DIFFERENT METHODS ON SPUCOANIMALS

The following commands and the hyperparameter ranges for various methods are provided below:

- **ERM:**

- Command: `python spuco_animals_erm.py`
- Hyperparameters:
 - * `lr = [1e-3, 1e-4, 1e-5]`
 - * `weight_decay = [1e-2, 1e-3, 1e-4]`

- **Group Balancing:**

- Command: `python spuco_animals_gb.py`
- Hyperparameters:
 - * `lr = [1e-3, 1e-4, 1e-5]`
 - * `weight_decay = [1e-2, 1e-3, 1e-4]`

- **GroupDRO:**

- Command: `python spuco_animals_gdro.py`
- Hyperparameters:
 - * `lr = [1e-3, 1e-4, 1e-5]`
 - * `weight_decay = [1e-2, 1e-3, 1e-4]`

- **EIIL:**

- Command: `python quickstart/spuco_animals/spuco_animals_eiil.py`
- Hyperparameters:
 - * `erm_lr = [1e-3, 1e-4]`
 - * `erm_weight_decay = [1e-3, 1e-4]`
 - * `gdro_lr = [1e-5, 1e-4]`
 - * `gdro_weight_decay = [1e-1, 1e-0]`
 - * `infer_num_epochs = [1, 2]`

Table 13: EIIL

	WATERBIRDS	CELEBA	URBANCARS
ERM LR	1e-3	1e-4	1e-4
ERM WD	1e-4	1e-4	1e-1
GDRO LR	1e-3	1e-5	1e-5
GDRO WD	1e-4	1e-1	1
Infer epoch	1	1	2
EIIL LR	1e-2	1e-3	1e-3
EIIL steps	20000	10000	20000
	SPUCoANIMALS	SPUCoSUN (Hard)	SPUCoSUN (Easy)
ERM LR	1e-3	1e-3	1e-3
ERM WD	1e-4	1e-3	1e-3
GDRO LR	1e-4	1e-4	1e-4
GDRO WD	1e-5	1e-4	1e-3
Infer epoch	2	2	1
EIIL LR	1e-3	1e-2	1e-2
EIIL steps	10000	10000	20000

Table 14: DFR

	WATERBIRDS	CELEBA	URBANCARS
ERM LR	1e-3	1e-4	1e-3
ERM WD	1e-3	1e-1	1e-1
	SPUCoANIMALS	SPUCoSUN (Hard)	SPUCoSUN (Easy)
ERM LR	1e-3	1e-3	1e-3
ERM WD	1e-4	1e-4	1e-4

```
* eiil_num_steps = [10000, 20000]
* eiil_lr = [1e-2, 1e-3]
```

- **SPARE:**

- Command: `python quickstart/spuco_animals/spuco_animals_spare.py`
- Hyperparameters:
 - * `erm_lr = [1e-3, 1e-4]`
 - * `erm_weight_decay = [1e-3, 1e-4]`
 - * `lr = [1e-3, 1e-4]`
 - * `weight_decay = [1e-1, 1e-2]`
 - * `infer_num_epochs = [1, 2]`
 - * `num_clusters = [2, 4]`
 - * `high_sampling_power = [1, 2]`

- **PDE:**

- Command: `python quickstart/spuco_animals/spuco_animals_pde.py`
- Hyperparameters:
 - * `lr = [1e-2, 1e-3, 1e-4]`
 - * `weight_decay = [1e-3, 1e-4]`
 - * `warmup_epochs = [15, 20]`
 - * `expansion_size = [10, 50]`
 - * `expansion_interval = [2, 10]`

- **JTT:**

- Command: `python spuco_animals_jtt.py`

Table 15: SSA

	WATERBIRDS	CELEBA	URBANCARS
SSL LR	1e-4	1e-5	1e-4
SSL WD	1e-1	1e-1	1
GDRO LR	1e-4	1e-4	1e-3
GDRO WD	1e-1	1	1e-4
	SPUCOANIMALS	SPUCOSUN (Hard)	SPUCOSUN (Easy)
SSL LR	1e-4	1e-2	1e-4
SSL WD	1e-3	1e-2	1e-5
GDRO LR	1e-3	1e-3	1e-4
GDRO WD	1e-4	1e-2	1e-3

- Hyperparameters:
 - * lr = [1e-3, 1e-4, 1e-5]
 - * weight_decay = [1e-5, 1e-4, 1e-3, 1e-2]
 - * num_epochs = [40, 100]
 - * infer_num_epochs = [1, 2]
- **DFR:**
 - Command: `python spuco_animals_dfr.py`
 - Hyperparameters:
 - * lr = [1e-3, 1e-4, 1e-5]
 - * weight_decay = [1e-5, 1e-4, 1e-3, 1e-2]
 - * num_epochs = [40, 100]
- **SSA:**
 - Command: `python spuco_animals_ssa.py`
 - Hyperparameters:
 - * infer_lr = [1e-2, 1e-3, 1e-4]
 - * infer_weight_decay = [1e-5, 1e-4, 1e-3, 1e-2]
 - * infer_num_iters = [1000, 45000]
 - * lr = [1e-3, 1e-4, 1e-5]
 - * weight_decay = [1e-5, 1e-4, 1e-3, 1e-2]
 - * num_epochs = [40, 100]



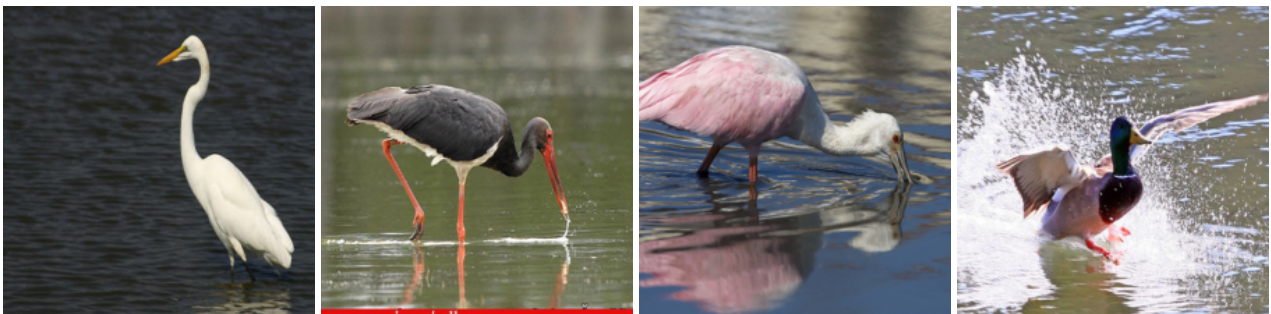
(a) Landbirds on Land



(b) Landbirds on Water

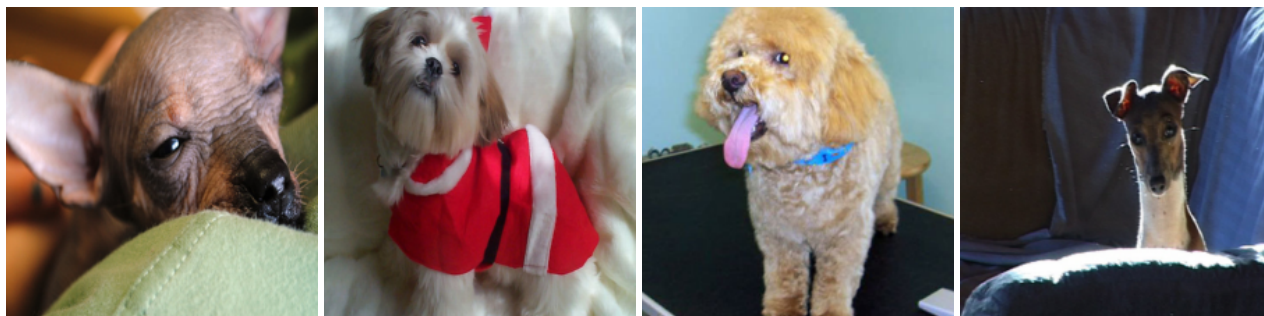


(c) Waterbirds on Land



(d) Waterbirds on Water

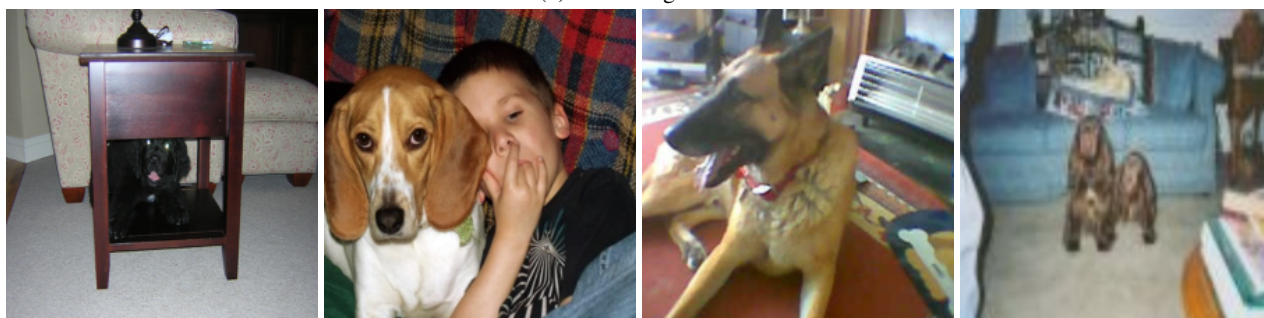
Figure 15: Examples from Bird Groups



(a) Small Dogs Indoor



(b) Small Dogs Outdoor



(c) Big Dogs Indoor



(d) Big Dogs Outdoor

Figure 16: Examples from Dog Groups

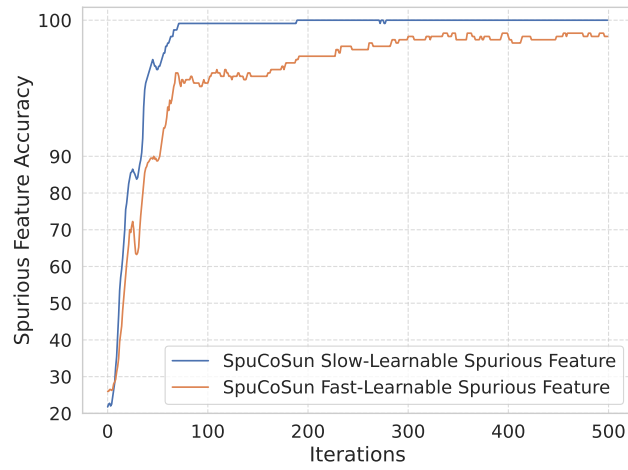


Figure 17: Comparing Average Accuracies of Majority and Minority Groups on SPUCoSUN (FAST) v/s SPUCoSUN

E.3 ADDITIONAL RESULTS ON THE CORRELATION BETWEEN GROUP INFERENCE PERFORMANCE AND WORST-GROUP ACCURACY

In this section, we evaluate the quality of inferred groups on the SPUCoSUN (EASY), SPUCoSUN (HARD), and URBAN-CARS datasets. A key distinction between these datasets and SPUCOANIMALS is that the former have a group-balanced validation set, while the validation set for SPUCOANIMALS mirrors the training set, containing a large majority group with a spurious feature. This difference in validation set distribution significantly increases the size of the minority group (examples without the class’s spurious feature) in the former datasets. As a result, group accuracy emerges as a more effective metric than minimum group precision for these datasets. Nonetheless, evaluating group inference on the validation set eliminates the need to train a model with inferred groups solely for tuning hyperparameters during the group inference stage of various methods. Thus, we continue to observe the significant cost savings due to the more efficient model selection offered by evaluation of inferred groups on the validation set.

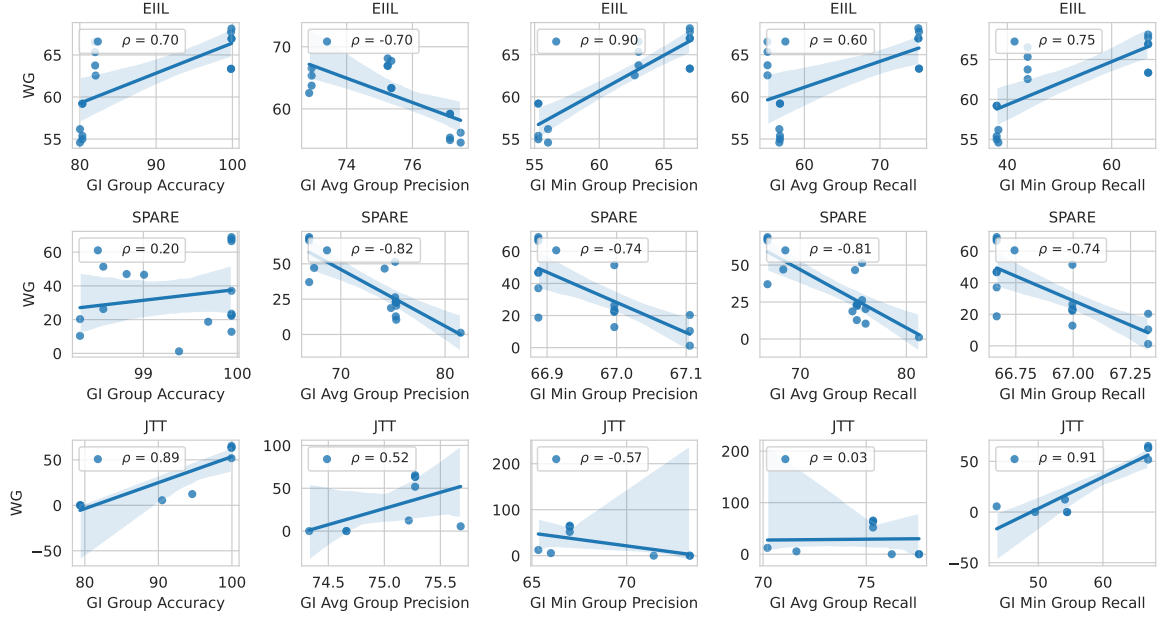


Figure 18: SPUCoSUN Easy

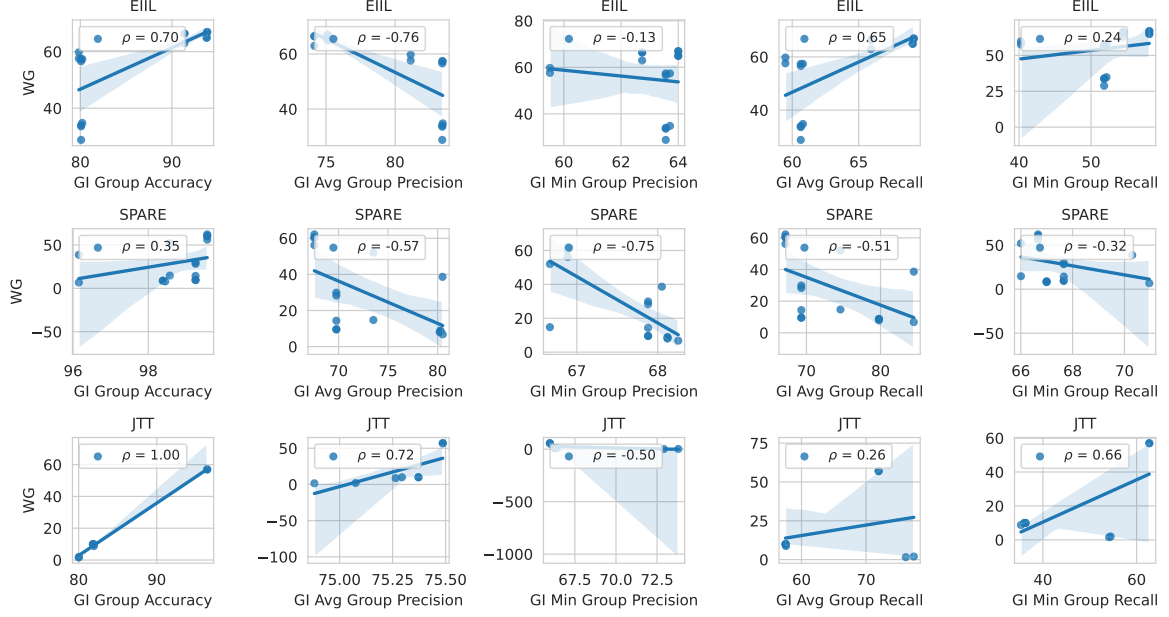


Figure 19: SPUCoSUN Hard

F ADDITIONAL RESULTS: PRETRAINED MODEL ARCHITECTURE

Here, we conduct an additional ablation study to assess the impact of architecture on the effectiveness of methods designed to mitigate spurious correlations. Our findings indicate that across all methods, including ERM, a Vision Transformer (ViT) pre-trained with CLIP consistently outperforms a ResNet-50 pre-trained with CLIP. This suggests that the increased number of parameters and/or the architecture of ViT contribute to enhanced robustness against spurious correlations.

Table 16: Performances of different methods with ViT.

	SPUCoSUN (Hard)		SPUCoSUN (Easy)	
	WG	Average	WG	Average
ERM	47.8	97.9	38.6	97.8
SPARE	86.1 ± 0.6	95.5 ± 0.5	84.7 ± 0.2	97.2 ± 0.3
EIIL	83.1 ± 0.1	90.9 ± 0.1	86.7 ± 0.1	94.7 ± 0.1
DFR	87.9 ± 0.3	94.3 ± 0.1	89.2 ± 0.1	92.9 ± 0.1
GB	77.7 ± 1.0	90.6 ± 0.5	78.9 ± 0.6	90.5 ± 0.1
PDE	89.2 ± 0.2	94.0 ± 0.5	87.5 ± 1.0	94.5 ± 0.1

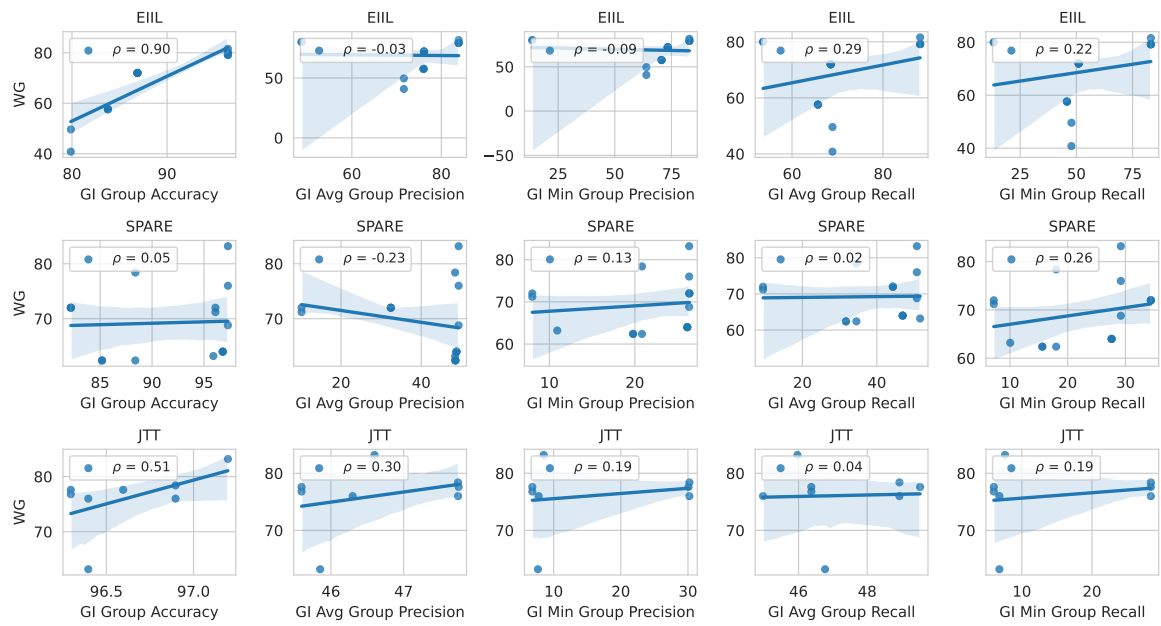


Figure 20: UrbanCars